

[View the Full Text HTML](#)



Nanosized Polymetallic Resorcinarene-Based Host Assemblies that Strongly Bind Fullerenes

O. Danny Fox,[†] James Cookson,[†] Emma J. S. Wilkinson,[†] Michael G. B. Drew,[‡] Elizabeth J. MacLean,[§] Simon J. Teat,[§] and Paul D. Beer^{*,†}

Contribution from the Department of Chemistry, University of Oxford, Inorganic Chemistry Laboratory, South Parks Road, Oxford, OX1 3QR, U.K., School of Chemistry, University of Reading, Whiteknights, Reading, Berks, RG6 6AD, and CCLRC Daresbury Laboratory, Daresbury, Warrington, Cheshire, WA4 4AD.

Received February 10, 2006; E-mail: paul.beer@chem.ox.ac.uk

Abstract: Polymetallic nanodimensional assemblies have been prepared via metal directed assembly of dithiocarbamate functionalized cavitand structural frameworks with late transition metals (Ni, Pd, Cu, Au, Zn, and Cd). The coordination geometry about the metal centers is shown to dictate the architecture adopted. X-ray crystallographic studies confirm that square planar coordination geometries result in “cagelike” octanuclear complexes, whereas square-based pyramidal metal geometries favor hexanuclear “molecular loop” structures. Both classes of complex are sterically and electronically complementary to the fullerenes (C₆₀ and C₇₀). The strong binding of these guests occurred via favorable interactions with the sulfur atoms of multiple dithiocarbamate moieties of the hosts. In the case of the tetrameric copper(II) complexes, the lability of the copper(II)–dithiocarbamate bond enabled the fullerene guests to be encapsulated in the electron-rich cavity of the host, over time. The examination of the binding of fullerenes has been undertaken using spectroscopic and electrochemical methods, electrospray mass spectrometry, and molecular modeling.

Introduction

Metal directed self-assembly is proving to be a versatile and efficient method for the construction of large and intricate three-dimensional supramolecular architectures of aesthetic appeal.¹ By judicious choice of metal and polydentate ligand components, the resulting self-assembled polymetallic molecular containers may exhibit unique redox, magnetic, and photochemical properties. Furthermore, such host systems have the ability to encapsulate and stabilize guest substrates, as well as catalyze chemical transformations within their “microreactor” cagelike structures.² The assembly of such molecules with labile metal ions is often a thermodynamically driven process, and as a consequence yields of self-assembled containers frequently

exceed those created by formation of covalent bonds. The field is currently dominated by polyhedral cluster structures, grids, ladders, and helicates resulting from metals in combination with a variety of oligopyridine and oligocatecholate ligands.³

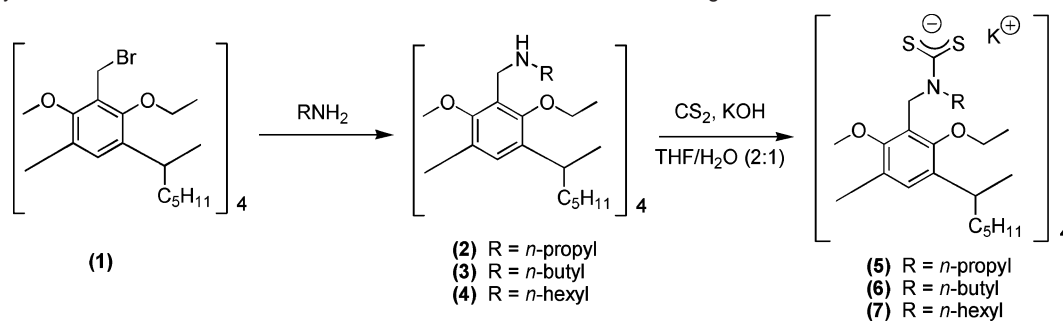
Chalice-shaped calixarene derivatives serve as excellent hosts for the binding of neutral and charged organic guest molecules. This has recently stimulated new pathways to multiple calixarene

[†] University of Oxford.

[‡] University of Reading.

[§] CCLRC Daresbury Laboratory.

- (1) (a) Fujita, M. *Chem. Soc. Rev.* **1998**, *27*, 417–425. (b) Caulder, D. L.; Raymond, K. N. *J. Chem. Soc., Dalton Trans.* **1999**, 1185–1200. (c) Leininger, S.; Olenyuk, B.; Stang, P. J. *Chem. Rev.* **2000**, *100*, 853–907. (d) Sauvage, J.-P. *Acc. Chem. Res.* **1998**, *31*, 611–619. (e) Saalfrank, R. W.; Demleitner, B. *Perspect. Supramol. Chem.* **1999**, *5*, 1–51. (f) Swiegers, G. F.; Malefetse, T. J. *Chem. Rev.* **2000**, *100*, 3483–3537. (g) Saalfrank, R. W.; Uller, E.; Demleitner, B.; Bernt, I. *Struct. Bonding* **2000**, *96*, 149–175. (h) Seidel, S. R.; Stang, P. J. *Acc. Chem. Res.* **2002**, *35*, 972–983. (i) Swiegers, G. F.; Malefetse, T. J. *Coord. Chem. Rev.* **2002**, *225*, 91–121. (j) Holliday, B. J.; Mirkin, C. A. *Angew. Chem., Int. Ed.* **2001**, *40*, 2022–2043. (k) Leininger, S.; Olenyuk, B.; Stang, P. J. *Chem. Rev.* **2000**, *100*, 853–908. (l) Tominga, M.; Suzuki, K.; Kawano, M.; Kusukawa, T.; Ozeki, T.; Sakamoto, S.; Yamaguchi, K.; Fujita, M. *Angew. Chem., Int. Ed.* **2004**, *43*, 5621–5625. (m) Fujita, M.; Tominaga, M.; Hori, A.; Therrien, B. *Acc. Chem. Res.* **2005**, *38*, 369–378. (n) Fiedler, D.; Leung, D. H.; Bergman, R. G.; Raymond, K. N. *Acc. Chem. Res.* **2005**, *38*, 349–358. (o) Schweiger, M.; Yamamoto, T.; Stang, P. J.; Blaser, D.; Boese, R. *J. Org. Chem.* **2005**, *70*, 4861–4864. (p) Xu, X.; Nieuwenhuyzen, M.; James, S. L. *Angew. Chem., Int. Ed.* **2002**, *41*, 764–768.
- (2) (a) Rebek, J. *Acc. Chem. Res.* **1999**, *32*, 278–286. (b) Sauvage, J. P. *Acc. Chem. Res.* **1998**, *31*, 611–619. (c) Fujita, M.; Fujita, N.; Ogura, K.; Yamaguchi, K. *Nature* **1999**, *400*, 52–55. (d) Merlau, M. L.; Meijja, M. P.; Nguyen, S. T.; Hupp, J. T. *Angew. Chem., Int. Ed.* **2001**, *40*, 4239–4242. (e) Paul, R. L.; Bell, Z. R.; Jeffery, J. C.; McCleverty, J. A.; Ward, M. D. *Proc. Natl. Acad. Sci. U.S.A.* **2002**, *99*, 4883–4888. (f) Bell, Z. R.; Harding, L. P.; Ward, M. D. *Chem. Commun.* **2003**, 2432–2433. (g) Yoshizawa, M.; Takeyama, Y.; Okano, T.; Fujita, M. *J. Am. Chem. Soc.* **2003**, *125*, 3243–3247. (h) Fiedler, D.; Pagliero, D.; Brumaghim, J. L.; Bergman, R. G.; Raymond, K. N. *Inorg. Chem.* **2004**, *43*, 846–848. (i) Leung, D. H.; Fiedler, D.; Bergman, R. G.; Raymond, K. N. *Angew. Chem., Int. Ed.* **2004**, *43*, 963–966. (j) Fielder, D.; Bergman, R. G.; Raymond, K. N. *Angew. Chem., Int. Ed.* **2004**, *43*, 6748–6751. (k) Argent, S. P.; Riis-Johannessen, T.; Jeffery, J. C.; Harding, L. P.; Ward, M. D. *Chem. Commun.* **2005**, 4647–4649.
- (3) (a) Tong, M. L.; Chen, H.-J.; Chen, X.-M. *Inorg. Chem.* **2000**, *39*, 2235–2238. (b) Biradha, K.; Seward, C.; Zaworotko, M. J. *Angew. Chem., Int. Ed.* **1999**, *38*, 492–495. (c) Wang, R.; Xu, L.; Ji, J.; Shi, Q.; Li, Y.; Zhou, Z.; Hong, M.; Chan, A. S. C. *Eur. J. Inorg. Chem.* **2005**, 751–758. (d) Lu, X.-Q.; Jiang, J.-J.; zur Loye, H.-C.; Kang, B.-S.; Su, C.-Y. *Inorg. Chem.* **2005**, *44*, 1810–1817. (e) Caulder, D. L.; Raymond, K. N. *Angew. Chem., Int. Ed. Engl.* **1997**, *36*, 1440–1442. (f) Fleming, J. S.; Mann, K. L. V.; Carrez, C.-A.; Psillakis, E.; Jeffery, J. C.; McCleverty, J. A.; Ward, M. D. *Angew. Chem., Int. Ed.* **1998**, *37*, 1279–1281. (g) Takeda, N.; Umemoto, K.; Yamaguchi, K.; Fujita, M. *Nature* **1999**, *398*, 794–796. (h) Breuning, E.; Ruben, M.; Lehn, J.-M.; Renz, F.; Garcia, Y.; Ksenofontov, V.; Gütllich, P.; Wegelius, E.; Rissanen, K. *Angew. Chem., Int. Ed.* **2000**, *39*, 2504–2507. (i) Ruben, M.; Breuning, E.; Lehn, J.-M.; Ksenofontov, V.; Renz, F.; Gütllich, P.; Vaughan, G. B. M. *Chem.-Eur. J.* **2003**, *9*, 4422–4429. (j) Lehn, J.-M.; Rigault, A. *Angew. Chem., Int. Ed. Engl.* **1988**, *27*, 1095–1097. (k) Baxter, P. N. W.; Hanan, G. S.; Lehn, J.-M. *Chem. Commun.* **1996**, 2019–2020. (l) Carina, R. F.; Dietrich-Buchecker, C.; Sauvage, J.-P. *J. Am. Chem. Soc.* **1996**, *118*, 9110–9116.

Scheme 1. Synthesis of Tetrakis-dithiocarbamate Functionalized Resorcinarene Building Blocks

container structures employing covalent,⁴ hydrogen-bonding⁵ and metal directed self-assembly⁶ synthetic techniques. Examples to date of metal coordinated calixarene based systems have been restricted to dimeric polymetallic species, including positively charged cavitand-based platinum(II) and palladium(II) nitrile- and pyridyl-coordination cages, which can encapsulate anions.⁷ Similarly, analogous cobalt(II) and iron(II) iminodiacetate cavitand dimers bind small aromatic and aliphatic guests in aqueous solution.⁸

While the coordination chemistry of the dithiocarbamate (dtc) ligand has been extensively documented,⁹ its application in the field of self-assembly is only now being realized.¹⁰ The ability of this ligand to stabilize metal ions in a range of oxidation states and coordination geometries offers plenty of opportunity for the generation of novel self-assembled molecular architectures with unique host-guest properties. Herein, we report in detail the preparation and characterization of a wide selection of transition metal dependent polymetallic dithiocarbamate nanosized host structures, including a new X-ray crystal structure of one of them.¹¹ In addition spectroscopic, electrospray mass spectrometry (ESMS), and electrochemical evidence together

with molecular modeling investigations reveal that these novel polymetallic assemblies strongly bind nanosized fullerene guest species.

Results and Discussion

Cavitand-Dithiocarbamate Ligand Synthesis. The respective tetrakis-dithiocarbamate functionalized cavitand ligands **5–7** were prepared by reaction of the parent resorcinarene secondary amines **2–4** in THF/water (2:1) with carbon disulfide and potassium hydroxide. The resorcinarene secondary amines **2–4** were prepared by treatment of the bromomethyl cavitand derivative **1**¹² with excess amounts of an appropriate amine (Scheme 1).

Although the potassium salts could be isolated, in all cases, polymetallic dtc cavitand complexes were prepared in a simple one-pot procedure by reaction of “in situ” formed **5–7** with transition metal salts.¹¹

Copper(II) – Directed Assembly of Resorcinarene Octanuclear Architectures. The novel tetrameric resorcinarene octanuclear copper(II) complexes **8–10** were prepared in good yields by reaction of **5–7** formed in situ from the parent amines **2–4** and excess copper(II) acetate and purified by recrystallization from dichloromethane/ethanol solvent mixtures (Scheme 2). All copper(II) assemblies were characterized by electrospray mass spectrometry, (vide infra) elemental analysis, and, in one case, single-crystal X-ray crystallography.

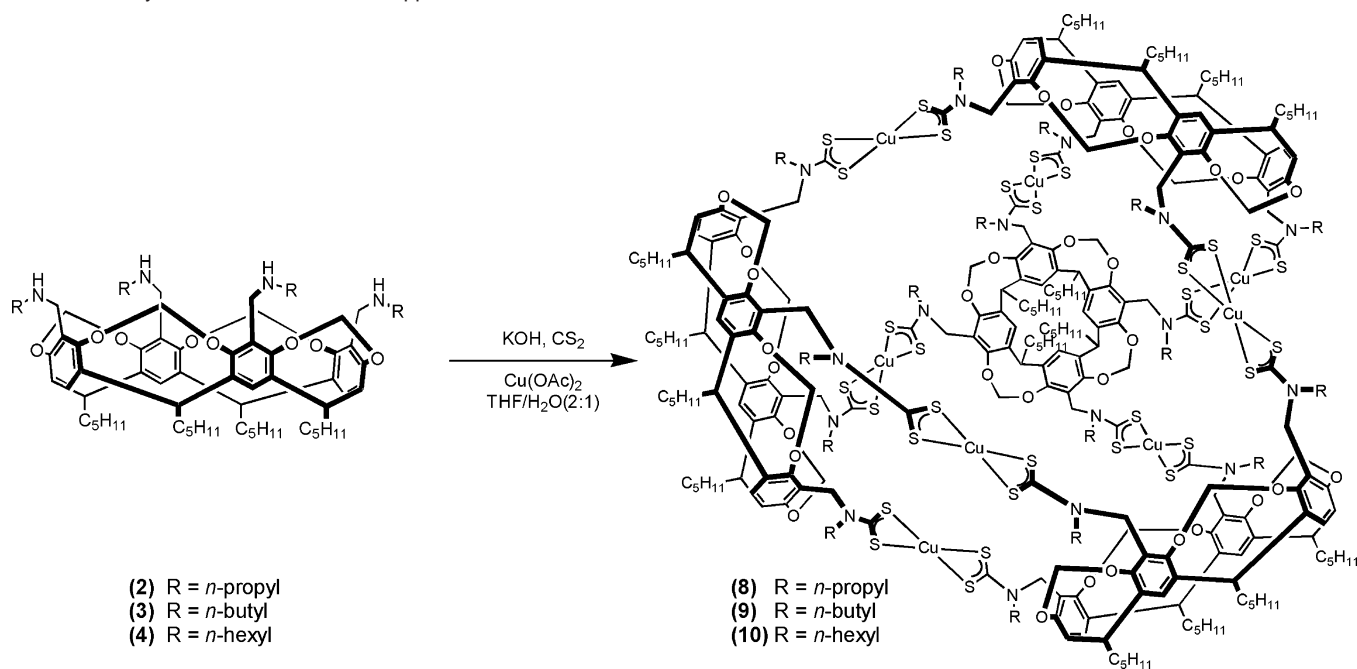
X-ray Crystallographic Characterization Of Copper(II) Resorcinarene Tetramer (10). Dark brown crystals of **10** were obtained by layering a solution of **10** in dichloromethane with ethanol and leaving it to stand for 2 months. Due to the size and complexity of **10** our initial attempts to determine the structure of this compound employing a diffractometer equipped with a Mar Research image plate and a sealed source X-ray tube were unsuccessful. The structure was eventually determined and solved employing the Synchrotron Radiation Source at the CCLRC Daresbury Laboratory (U.K.).

The resulting structure demonstrates the adoption of the novel cagelike octanuclear architecture in the solid state. The resorcinarene subunits form the corners of a pseudo-tetrahedral structure. To form this array, geometrical requirements dictate that at two sides of the tetrahedron two copper centers are coordinated to the same resorcinarene, with overall crystallographic *S*₄ symmetry (Figure 1). The gross structural effect of this is to distort the symmetry of the molecule, twisting the cups of the resorcinarenes away from the line of the apexes,

- (4) (a) Jasat, A.; Sherman, J. C. *Chem. Rev.* **1999**, *99*, 931–968. (b) Cram, D. J.; Tanner, M. E.; Thomas, R. *Angew. Chem., Int. Ed. Engl.* **1991**, *30*, 1024–1027. (c) Barrett, E. S.; Irwin, J. L.; Edwards, A. J.; Sherburn, M. S. *J. Am. Chem. Soc.* **2004**, *126*, 16747–16749.
- (5) (a) MacGillivray, L. R.; Atwood, J. L. *Nature* **1997**, *389*, 469–472. (b) Gerkenmeier, T.; Iwanek, W.; Agena, C.; Frohlich, R.; Kotila, S.; Nather, C.; Mattay, J. *Eur. J. Org. Chem.* **1999**, 2257–2262. (c) Atwood, J. L.; Barbour, L. J.; Jerga, A. J. *Supramol. Chem.* **2001**, *1*, 131–134. (d) Heinz, T.; Rudkevich, D. M.; Rebek, J., Jr. *Nature* **1998**, *394*, 764–766. (e) Kobayashi, K.; Shirasaka, T.; Yamaguchi, K.; Sakamoto, S.; Horn, E.; Furukawa, N. *Chem. Commun.* **2000**, 41–42.
- (6) (a) Fujimoto, K.; Shinkai, S. *Tetrahedron Lett.* **1994**, *35*, 2915–2918. (b) Jacopozzi, P.; Dalcanele, E. *Angew. Chem., Int. Ed. Engl.* **1997**, *36*, 613–615.
- (7) (a) Pirondini, L.; Bertolini, F.; Cantadori, B.; Ugozzoli, F.; Massera, C.; Dalcanele, E. *PNAS* **2002**, *99*, 4911–4915. (b) Fochi, F.; Jacopozzi, P.; Wegelius, E.; Riassanen, K.; Cozzini, P.; Marastoni, E.; Fiscaro, E.; Manini, P.; Fokkens, R.; Dalcanele, E. *J. Am. Chem. Soc.* **2001**, *123*, 7539–7552. (c) Pinalli, R.; Cristini, V.; Sottili, V.; Geremia, S.; Campagnolo, M.; Caneschi, A.; Dalcanele, E. *J. Am. Chem. Soc.* **2004**, *126*, 6516–6517.
- (8) (a) Fox, O. D.; Dalley, N. K.; Harrison, R. G. *J. Am. Chem. Soc.* **1998**, *120*, 7111–7112. (b) Fox, O. D.; Dalley, N. K.; Harrison, R. G. *Inorg. Chem.* **1999**, *38*, 5860–5863. (c) Fox, O. D.; Leung, J. F.-Y.; Hunter, J. M.; Dalley, N. K.; Harrison, R. G. *Inorg. Chem.* **2000**, *39*, 783–790.
- (9) (a) Coucouvanis, D. *Prog. Inorg. Chem.* **1979**, *26*, 301–469. (b) Hogarth, G. *Prog. Inorg. Chem.* **2005**, *53*, 71–560.
- (10) (a) Beer, P. D.; Berry, N. G.; Drew, M. G. B.; Fox, O. D.; Padilla-Tosta, M. E.; Patell, S. *Chem. Commun.* **2001**, 199–200. (b) Uppadine, L. H.; Weeks, J. M.; Beer, P. D. *J. Chem. Soc., Dalton Trans.* **2001**, 3367–3372. (c) Webber, P. R. A.; Drew, M. G. B.; Hibbert, R.; Beer, P. D. *J. Chem. Soc., Dalton Trans.* **2004**, 1127–1135. (d) Wong, W. W. H.; Cookson, J.; Evans, E. A. L.; McInnes, E. J. L.; Wolowska, J.; Maher, J. P.; Bishop, P.; Beer, P. D. *Chem. Commun.* **2005**, 2214–2216. (e) Wilton-Ely, J. D. E. T.; Solanki, D.; Hogarth, G. *Eur. J. Inorg. Chem.* **2005**, 4027–4030.
- (11) Part of this work has been published as preliminary communications: (a) Fox, O. D.; Drew, M. G. B.; Beer, P. D. *Angew. Chem., Int. Ed.* **2000**, *39*, 136–140. (b) Fox, O. D.; Wilkinson, E. J. S.; Beer, P. D.; Drew, M. G. B. *Chem. Commun.* **2000**, 391–392.

- (12) Boerigter, H.; Verboom, W.; Reinhoudt, D. N. *J. Org. Chem.* **1997**, *62*, 7148–7155.

Scheme 2. Synthesis of Octanuclear Copper Architectures



resulting in a flattening of the tetrahedron. The average Cu–S bond length in the structure is 2.29 Å and is typical for copper(II) alkyldithiocarbamate complexes.¹³ The overall complexity of **10** is in part due to the presence of two distinct octanuclear copper(II) resorcinarene tetramers, resulting in 16 crystallographically unique copper(II) centers in the unit cell.

The octanuclear copper(II) resorcinarene complexes **8–10** can be oxidized with iodine in dichloromethane–toluene solutions to yield the corresponding copper(III) complexes. On slow evaporation of an oxidized solution of **8**, small dark brown prismatic crystals of the copper(III) complex were isolated, which were suitable for single-crystal X-ray structural analysis. This previously reported structure,^{11a} [Cu₈{(5)-4K}₄][I₃]₇[I]·6H₂O (**8***), is also an octanuclear structure with an approximate S₄ axis and a tetrahedral cavity. The geometry of the copper coordination spheres is approximately square planar in both **10**

and **8***. However, there are significant differences in the geometry of the tetramer, which is apparent in Figure 2 but is emphasized in Figure 3 that compares the geometry of the two copper networks. For example, the distance between the central copper atoms (shown as *c* in Figure 3) is very much smaller in **10** at 4.98 Å than in **8*** where it is 7.08 Å. Concomitant with this difference is distance *d*, which is 14.17 Å in **10** and 16.43 Å in **8***. The remaining dimensions are similar in the two structures.

Solution Phase Characterization of Octanuclear Copper Tetramers. There is considerable evidence demonstrating that the copper dithiocarbamate complexes also adopt an octanuclear structure in solution, as well as in the solid state. Addition of oxidants to solutions of the brown copper(II) complexes **8–10** resulted in the generation of green solutions. This color change was monitored using UV–vis spectroscopy for the addition of copper(II) triflate to a dichloromethane solution of **8** (Figure 4). This resulted in regular increases in absorption up to the addition of 8 equiv of the oxidant. Further addition did not result in any significant change in the electronic spectra. This illustrates that the copper complex is also octanuclear in solution, and the smooth oxidation agrees with the X-ray analyses that there is no significant structural rearrangement upon oxidation.

Electrospray mass spectrometry (ESMS) has also been used to confirm that the octanuclear resorcinarene structure is maintained in solution. The detection of this was assisted by chemical oxidation prior to ESMS analysis.¹⁴ Using either copper(II) triflate or nitrosium tetrafluoroborate as an oxidant, a series of multiply charged peaks corresponding to the formation of tetramer adducts with a varying number of triflate

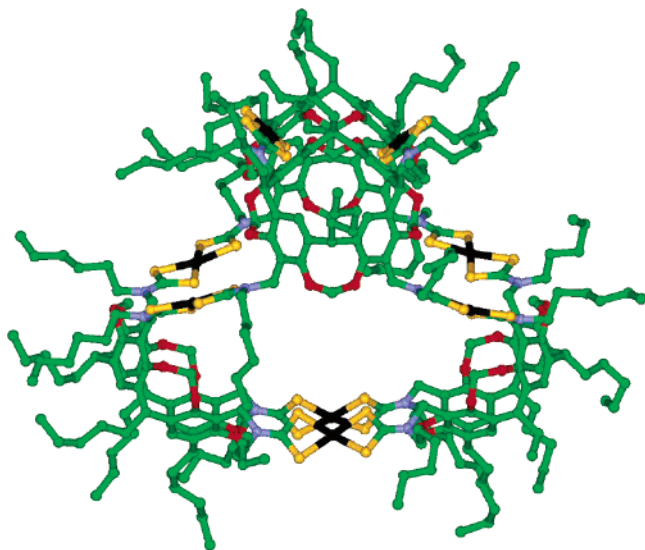


Figure 1. View of the structure of **10** which has crystallographic S₄ symmetry about the central cavity of the complex. Black, copper; dark yellow, sulfur; blue, nitrogen; red, oxygen; green, carbon.

(13) Jian, F.; Wang, Z.; Bai, Z.; You, X.; Fun, H.-K.; Chinnakali, K.; Razak, I. A. *Polyhedron* **1999**, *18*, 3401–3406.

(14) (a) Bond, A. M.; Martin, R. L. *Coord. Chem. Rev.* **1984**, *54*, 23–98. (b) Bond, A. M.; Colton, R.; D'Agostino, A.; Harvey, J.; Traeger, J. C. *Inorg. Chem.* **1993**, *32*, 3952–3956. (c) Bond, A. M.; Colton, R.; Traeger, J. C.; Harvey, J. *Inorg. Chim. Acta* **1993**, *212*, 233–238. (d) Bond, A. M.; Colton, R.; Gatehouse, B. M.; Mah, Y. A. *Inorg. Chim. Acta* **1997**, *260*, 61–71.

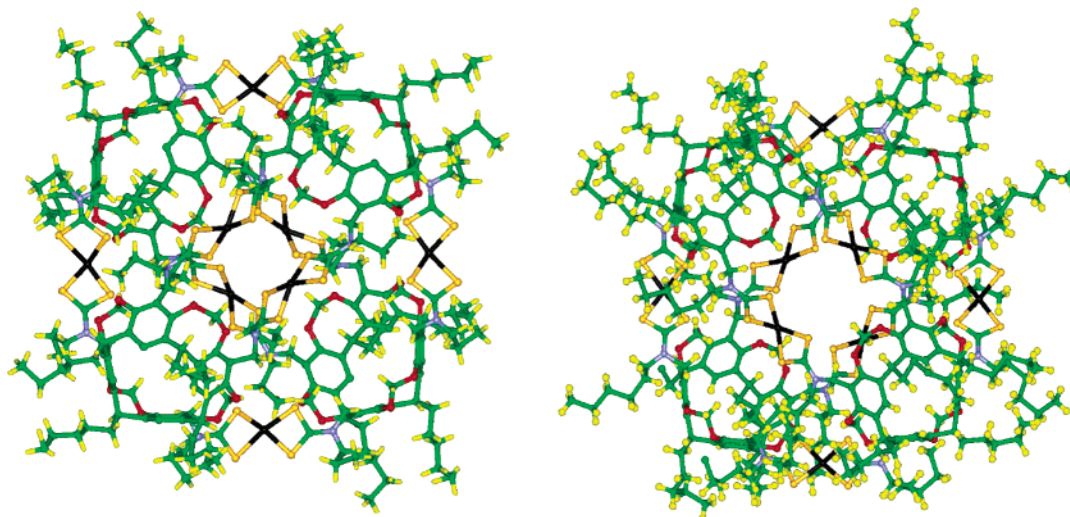


Figure 2. Structures of **10** and **8*** looking down the crystallographic S_4 axis in **10** (left) and the approximate S_4 axis in **8*** (right). Black, copper; dark yellow, sulfur; blue, nitrogen; red, oxygen; green, carbon; yellow, hydrogen.

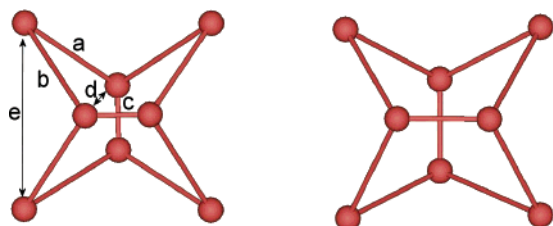


Figure 3. Arrangement of the eight copper atoms in **10** (left) and **8*** (right). Distances in **10** which has crystallographic S_4 symmetry are as follows: (a) 11.52, (b) 10.38, (c) 4.99, (d) 14.17, (e) 14.36 Å. In **8*** which has no imposed symmetry, the average distances are as follows: (a) 11.36, (b) 11.45, (c) 7.08, (d) 16.43, (e) 14.74 Å.

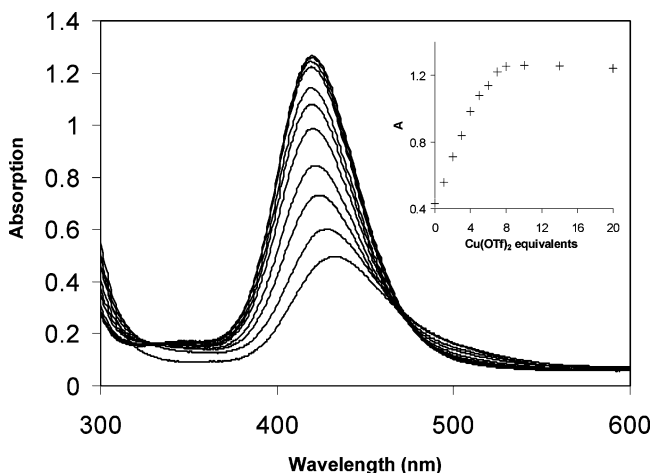


Figure 4. Electronic spectrum of **8** in CH_2Cl_2 upon the addition of $\text{Cu}(\text{OTf})_2$. Inset: the increase in absorbance at 418 nm after the addition of given equivalents of oxidant.

or tetrafluoroborate counteranions was observed by ESMS (Figure 5). This is confirmed by the excellent match of the peaks with the predicted isotopic patterns. These experiments were performed under ambient temperatures and cone voltages, which, in combination with the in situ oxidation of the metal centers, resulted in significantly higher ion counts.

Due to the paramagnetic nature of the copper(II) nucleus it was not possible to obtain NMR spectra of the octanuclear complexes. However, addition of excess NOBF_4 in $\text{CDCl}_3/\text{CD}_3\text{-CN}$ (1:1) solution generated the diamagnetic copper(III) species,

allowing the ^1H NMR spectrum to be recorded (refer to Supporting Information). The spectrum displays peaks characteristic of the resorcinarene cavitand ligands, although they are broad in nature. The spectrum does appear more complicated than that for the corresponding parent amine **2**. For instance, the aromatic protons are observed as two broad singlets at 7.31 and 7.35 ppm, and the outer bridging methylene protons are seen as a broad multiplet centered at 5.80 ppm. The lack of clarity for these signals is possibly a result of the structure of the complex, with the X-ray crystal structure of both the copper(II) and copper(III) dithiocarbamate based resorcinarene complexes existing as a flattened tetrahedron in the solid state. If the same flattened tetrahedral structure was adopted in solution, then it would be expected that these two signals would appear doubled, as they would exist in two different environments. As this is the case, this is further evidence that an octanuclear structure is also adopted in solution.

Zinc(II) and Cadmium(II) Resorcinarene Trimeric Structures. The in situ synthetic procedure to produce the tetrakis-dithiocarbamate salts **5–7** followed by addition of zinc(II) and cadmium(II) acetate afforded cream powders. Recrystallization of these from pyridine–water solutions afforded yellow prismatic crystals, pyridine adducts of novel hexanuclear structures **11–16** in yields between 51 and 62% (Scheme 3).

Four compounds were characterized by single-crystal X-ray crystallography and have been reported in a preliminary communication.¹¹ The structures are isomorphous and consist of three resorcinarene cups linked by six divalent metal ions all of which are crystallographically equivalent. The cup-shaped resorcinarene ligands provide the corners of an equilateral molecular triangle whose sides are ca. 19–20 Å in length. The curve in the structure is a result of the zinc and cadmium centers adopting a pyramidal five-coordinate geometry, with the pyridine donor occupying the axial site. The structure of **11** is highlighted in Figure 6, and selected parameters of the structures given in Table 1.

Although the ^1H NMR spectra of **11–16** in d_8 -toluene are broad, they do exhibit resonances characteristic of the resorcinarene ligands. The broad nature of the peaks is probably due to the large size of the structure and to conformational mobility within the polymetallic assembly, such as the slow rotational

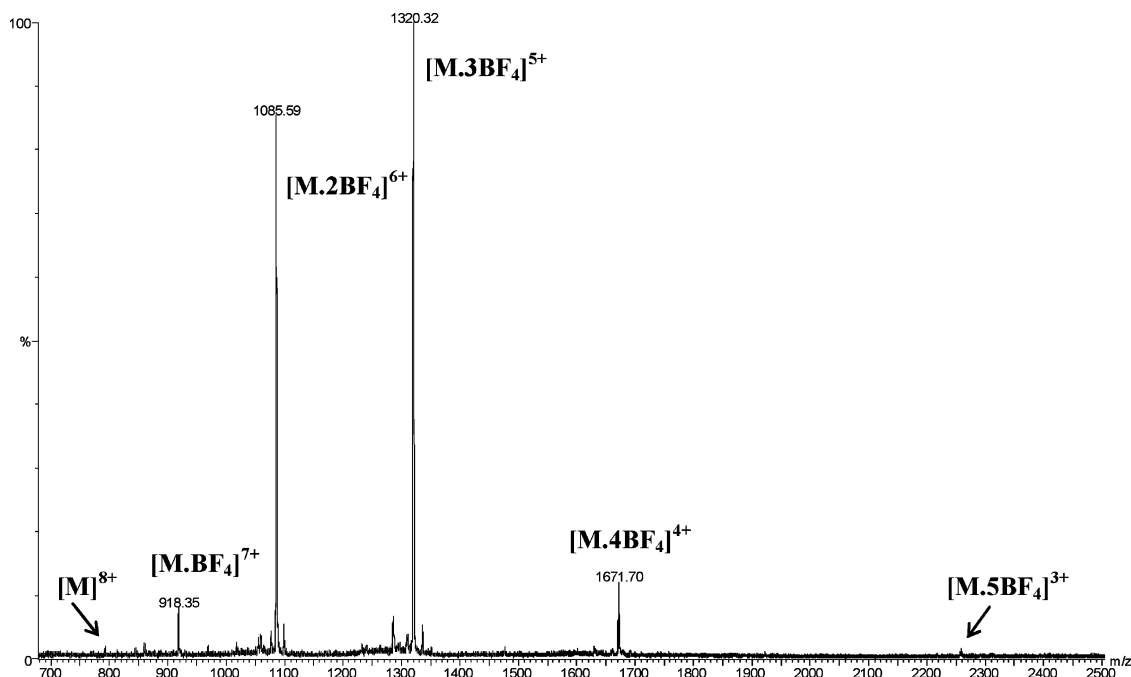
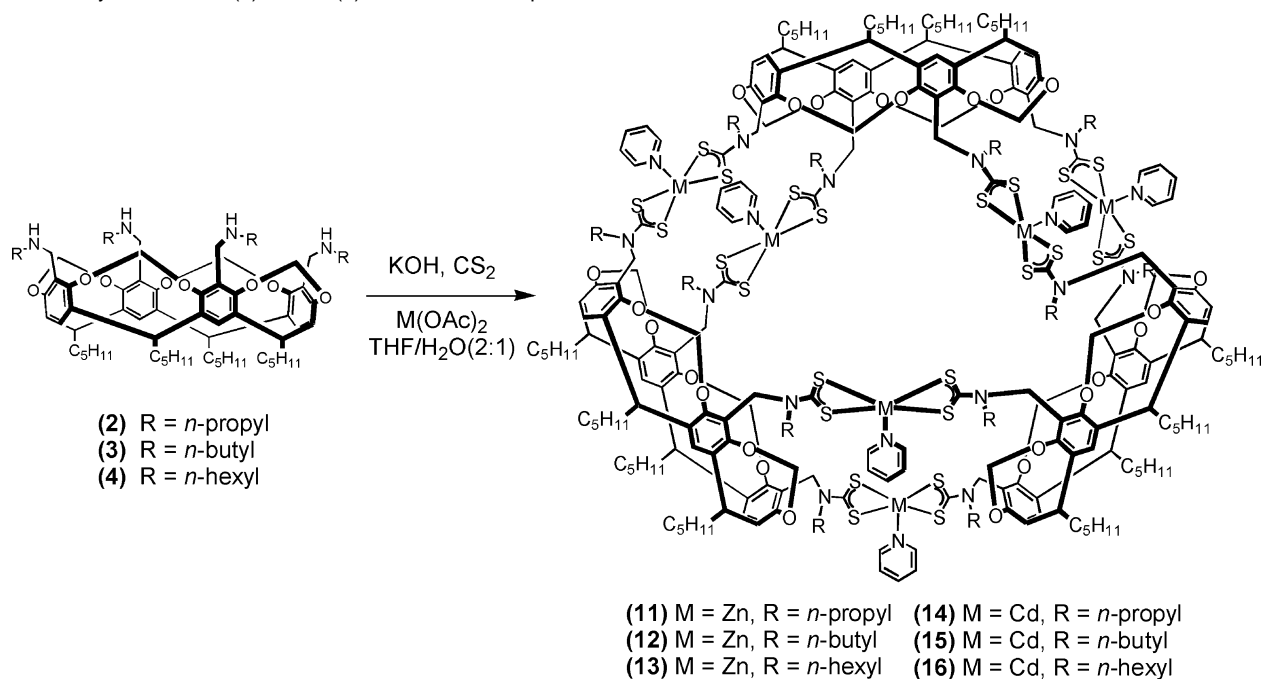


Figure 5. Electrospray mass spectrum of **9** via in situ oxidation with NOBF_4 .

Scheme 3. Synthesis of Zn(II) and Cd(II) Hexanuclear Loop Structures



processes around the C–N bonds of the metal-dtc units. Unfortunately, attempts to elucidate the structure via both ESMS and MALDI-TOF mass spectrometry proved inconclusive, with only fragments of the hexanuclear structures being observed. However, the propensity of the complexes to strongly bind fullerene guest species provides evidence for these hexametallc molecular loop structures existing in solution (vide infra).

Gold(III) Resorcinarene Complexes. Initially the synthesis of a gold(III) dithiocarbamate functionalized resorcinarene assembly (**17**) was attempted by a “one-pot” reaction with the tetrakis-amine **2**, potassium hydroxide, carbon disulfide, and hydrogen tetrachloroaurate in aqueous THF (Scheme 4). Analysis of the resulting brown solution using ESMS revealed the

presence of an octanuclear gold(III) dtc complex (**17**), although this was accompanied by numerous byproducts from which it proved impossible to separate.

A transmetalation reaction was undertaken in which an excess of HAuCl_4 was added to a dichloromethane/acetonitrile (1:1) solution of the octanuclear copper(II) dtc octanuclear complex **9**. A rapid color change from brown to golden yellow was observed. The ESMS spectrum of the resulting mixture (Figure 7) shows that addition of HAuCl_4 to the octanuclear complex results in the rapid displacement of all eight copper(II) metal centers for gold(III). The product is the same through the transmetalation route as it is from the direct reaction from the

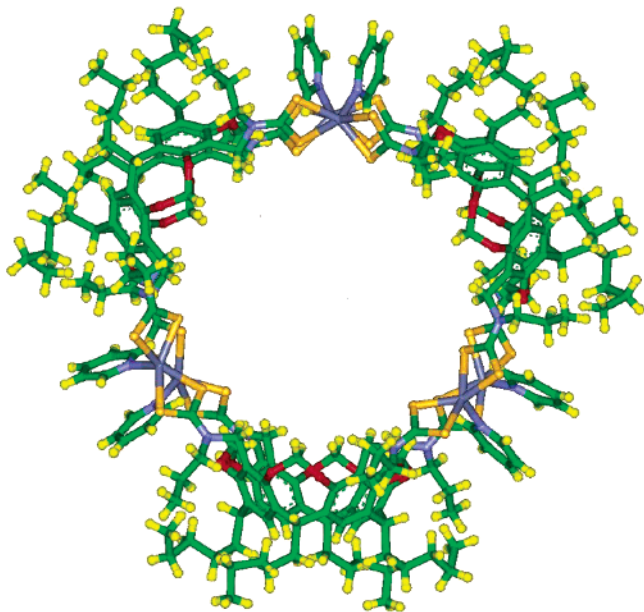


Figure 6. X-ray crystal structure of **11**. Dark blue, Zn; dark yellow, sulfur; blue, nitrogen; red, oxygen; green, carbon; yellow, hydrogen.

Table 1. Structural Parameters for Hosts **11**, **12**, **14**, and **15**

host	M···M(adj) ^a (Å)	M···M(opp) ^b (Å)	cavity dimensions ^c (Å)
11	6.61	14.69	19.13
12	6.65	14.59	19.18
14	6.73	14.72	19.59
15	6.74	14.65	19.58

^a Distance between adjacent metal centers. ^b Distance between opposite metal centers (i.e., across the cavity). ^c Dimensions of the cavity as defined by carbon atoms at the base of the resorcinarene.

parent amine (Scheme 4). It is noteworthy that, via this transmetalation route, no significant amounts of byproducts were observed.

The resultant complex is stabilized by the formation of adducts with excess tetrachloroaurate anion. It is possible that these anions may be situated within the central cavity of the cage-like structure. Such an interaction may well be necessary to maintain the structure, as in its absence the mutual electrostatic repulsion between the positively charged gold(III) centers within the structure may result in its instability. Despite the presence of these stabilizing counteranions within the architecture, rerecording the ESMS after 10 min revealed that the assembly had decomposed. Attempts to isolate the octanuclear complex via the addition of 8 equiv or an excess of tetrachloroaurate proved unsuccessful.

An analogous transmetalation reaction was also attempted using the hexanuclear zinc(II) trimeric complex **12**. Analysis by ESMS of the resulting solution mixture did not reveal the presence of any nanodimensional products, with only fragmentation peaks being observed.

Group 10 Dithiocarbamate Resorcinarene Assemblies. The in situ synthesis of **6** followed by addition of nickel(II) acetate, potassium tetrachloropalladate, and tetrachloroplatinate afforded green, yellow, and red solid products, respectively. The platinum derivative proved insoluble in all common organic solvents, while the nickel(II) (**18**) and palladium(II) (**19**) complexes were purified by recrystallization from dichloromethane/ethanol

solvent mixtures. Although single crystalline samples of both complexes failed to produce diffraction data upon X-ray analysis, elemental analytical data were consistent with respective metal dtc resorcinarene complexes. The use of ESMS and MALDI-TOF mass spectrometry only gave fragmentation peaks; however, both complexes were found to be diamagnetic, enabling ¹H NMR spectra to be scrutinized. The resulting temperature-independent, broad spectra display peaks corresponding to those expected for the resorcinarene framework. Interestingly, however, the OCH₂ peaks do not appear as the two doublets, which are observed in the parent resorcinarene **3**; instead a number of peaks are observed (refer to Supporting Information).

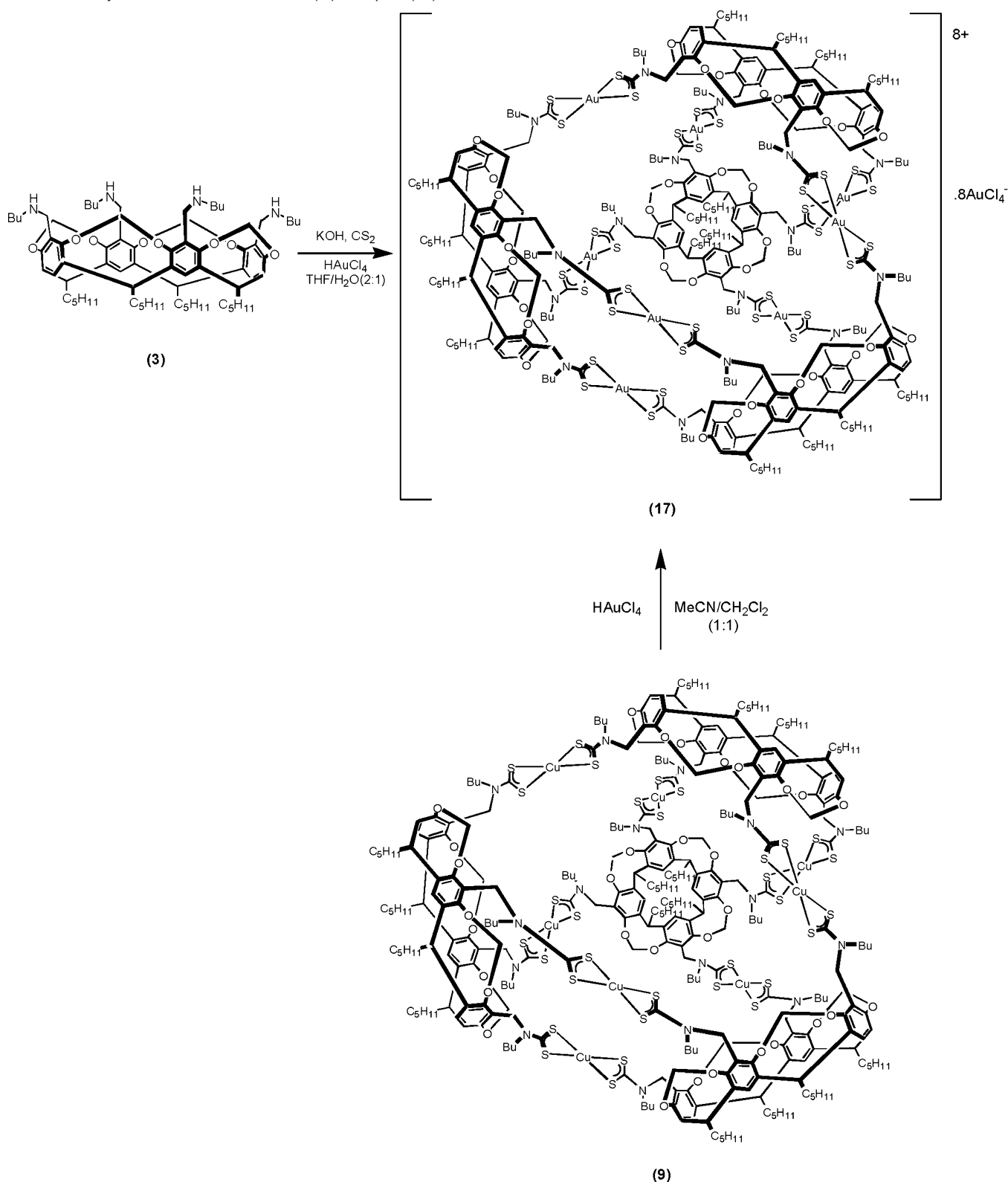
The increased complexity of the OCH₂ area of the spectra is possibly due to the occurrence of more than one environment of these protons within the complexes. This may imply the formation of an unsymmetrical structure, such as the flattened tetrahedron, as observed for the copper complexes. It is unlikely that lower nuclearity complexes would give rise to this feature since it would be expected that dimer or trimer formation would result in symmetrical environments for these protons. There are further factors that make it likely that the nickel(II) and palladium(II) systems adopt similar octanuclear structures as the copper(II) complexes. Simple acyclic copper(II), nickel(II), palladium(II), and gold(III) dialkyl-dtc complexes are all known to adopt the same square planar geometry about the central metal ion. As discussed in the previous section, gold(III) dithiocarbamate resorcinarene complexes have been shown from ESMS investigations to form tetrameric structures both from metal-directed self-assembly of **3** and from transmetalation reactions of the corresponding copper(II) octanuclear complex **9**. This suggests that the tetrameric structure is the thermodynamically favored structure for metal cations with square planar geometric preferences. It is therefore likely that the nickel(II) and palladium(II) complexes **18** and **19**, by analogy, also adopt an octanuclear tetrahedral structure.

Fullerene Binding Investigations with Zinc and Cadmium Hexanuclear Assemblies. Since their discovery in 1985, buckminsterfullerene and its related fullerenes have generated diverse, rapidly growing and active research areas ranging from superconductivity to biological activity.¹⁵ There has also been significant exploration in the supramolecular chemistry of fullerenes.¹⁶ For example, electron-rich π -systems, such as calixarenes, cyclotrimeratrylene (CTV) derivatives, and modified porphyrins have been shown to form strong inclusion complexes with fullerenes resulting from steric and electronic host–guest fullerene complementarity.¹⁷ The cadmium and zinc dtc hexanuclear resorcinare architectures contain central cavities of complementary nanosized dimensions to fullerenes C₆₀ and C₇₀. Preliminary binding investigations revealed purple solutions of

(15) *Fullerenes: Chemistry, Physics, and Technology*; Kadish, K. M., Ruoff, R. S., Eds.; Wiley-Interscience: New York, 2000.

(16) Diederich, F.; Gomez-Lopez, M. *Chem. Soc. Rev.* **1999**, *28*, 263–278.

(17) (a) Atwood, J. L.; Barbour, L. J.; Heaven, M. W.; Raston, C. L. *Chem. Commun.* **2003**, 2270–2271. (b) Atwood, J. L.; Barnes, M. J.; Gardiner, M. G.; Raston, C. L. *Chem. Commun.* **1996**, 1449–1451. (c) Ikeda, A.; Udzu, H.; Yoshimura, M.; Shinkai, S. *Tetrahedron* **2000**, *56*, 1825–1832. (d) Sun, D. Y.; Tham, F. S.; Reed, C. A.; Chaker, L.; Boyd, P. D. W. *J. Am. Chem. Soc.* **2002**, *124*, 6604–6612. (e) Shirakawa, M.; Fujita, N.; Shinkai, S. *J. Am. Chem. Soc.* **2003**, *125*, 9902–9903. (f) Shoji, Y.; Tashiro, K.; Aida, T. *J. Am. Chem. Soc.* **2004**, *126*, 6570–6571. (g) Kieran, A. M.; Pascu, S. I.; Jarrosson, T.; Sanders, J. K. M. *Chem. Commun.* **2005**, 1276–1278. (h) Sun, Y.; Drovetskaya, T.; Bolksar, R. D.; Bau, R.; Boyd, P. D. W.; Reed, C. A. *J. Org. Chem.* **1997**, *62*, 3642–3649. (i) Dudic, M.; Lhoták, P.; Stibor, I.; Petricková, H.; Lang, K. *New J. Chem.* **2004**, 85–90.

Scheme 4. Synthesis of Octanuclear Gold(III) Complex (17) via a Direct Reaction and a Transmetalation

C₆₀ in toluene or benzene turn red-brown on addition of colorless hexanuclear hosts **11–16**. Such a color change is indicative of a binding interaction between the host and the guest. UV–visible Job plot investigations¹⁸ determined a 1:1 binding stoichiometry between hosts and guests. Subsequent titration experiments and

Specfit analysis¹⁹ of fullerene titration experiments enabled association constants with C₆₀ and C₇₀ to be determined. Tables 2 and 3 display all the associated constants for both fullerene guests.

The stability constants indicate that binding is significantly stronger in benzene solution than in toluene. It is noteworthy

(18) Connors, K. A. *Binding Constants*; Wiley: New York, 1987.

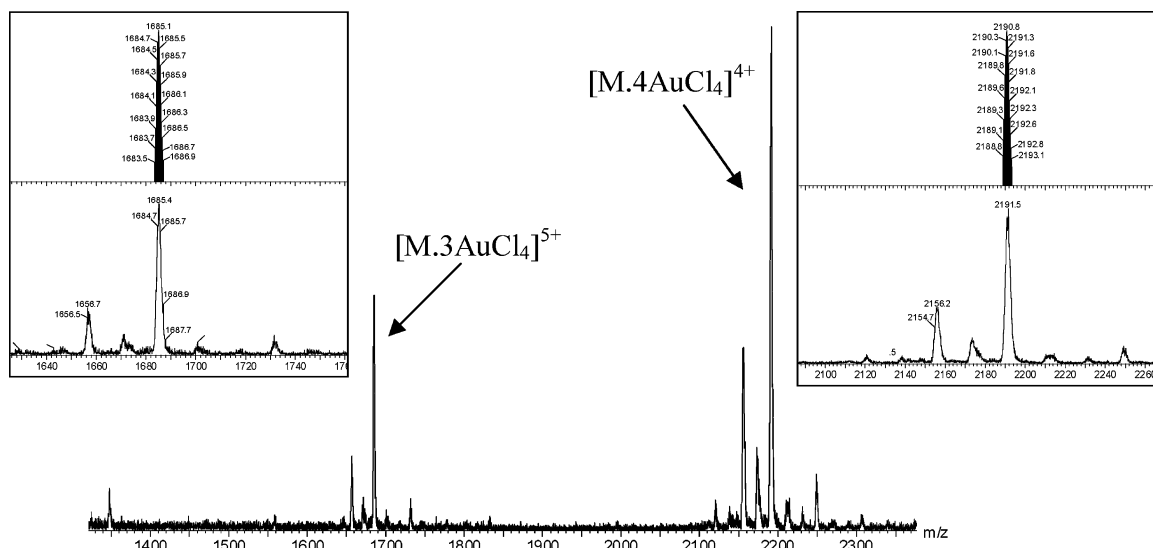


Figure 7. Electrospray mass spectrum of Au(III) complex **17** formed via the transmetalation of **9**.

Table 2. Association Constants (log *K*) for Host Structures and Guest C₆₀ Determined via UV–vis Spectroscopy

solvent	11	12	14	15
benzene	4.07	4.41	>6 ^a	4.7
toluene	3.47	3.70	5.1	4.3

^a *T* = 295 K, concentration of host receptor 1.07 × 10^{−4} M, errors < 10%.

Table 3. Association Constants (log *K*) for Host Structures and Guest C₇₀ Determined via UV–vis Spectroscopy^{b,c}

solvent	11	12	14	15
benzene	3.77	4.16	>6 ^a	4.2
toluene	3.55	4.03	4.7	4.0

^a *T* = 295 K, concentration of host receptor 5.035 × 10^{−5} M, errors < 10%. ^b Owing to the strength of binding, a satisfactory convergence in the fitting program could not be reached. ^c Potassium salts **5** and **6** were also titrated with C₆₀, and their UV–vis spectra recorded. However, in these cases there were no observed spectral changes, indicative of no interaction with the fullerene.

that the cadmium complexes **14** and **15** bind C₆₀ and C₇₀ much more strongly than their zinc analogues **11** and **12**, although the cavity dimensions of the respective hosts are very similar (Table 1), namely circular with an approximate diameter of 16–17 Å²⁰ (Figure 6). It is therefore unlikely that this modest difference in host size and shape can reasonably account for the large variation in association constant magnitudes observed. It is more likely that this is a result of the different electronic natures of the metal centers. This is also supported by the fact that addition of the potassium tetrakis-dithiocarbamate functionalized resorcinarene building blocks **5** and **6** did not perturb the electronic spectra of C₆₀, implying that the binding process occurs via the metal-dtc bonds. Molecular modeling of the interaction of C₆₀ with these hosts is discussed further (vide infra).

The binding of C₇₀ by the zinc and cadmium architectures displays the same trends as those for the smaller fullerene. This suggests that the same mode of association is occurring in the binding of both fullerenes. The association constants are in general lower for the larger fullerene, implying a preference

for binding C₆₀ over C₇₀. This difference is not, however, as marked as those observed in calix[8]arene.^{21,22}

¹³C NMR has previously been used to gauge the inclusion of fullerenes by calixarene and CTV-based hosts, by measuring the induced shifts of the fullerene guests. Encapsulation led to measurable upfield shifts (typically ~0.3 ppm) due to anisotropic shielding by the host.²³ It has been demonstrated that fullerenes also interact with hydrophobic cavities of the electron-rich γ -cyclodextrin (γ -CyD), in a (1:2) C₆₀– γ -CyD complex.²⁴ These complexes are primarily stabilized via charge-transfer interactions between C₃ and C₄ oxygen donors of the glucose subunits and the electron-deficient fullerene. The induced shift of these complexes has also been measured, and this has given rise to a downfield perturbation of 0.82 ppm in the ¹³C NMR signal of C₆₀. The differing nature of these shifts is indicative of the nature of the different mode of binding host and guest.

Due to its symmetry, C₆₀ exhibits one peak in its ¹³C NMR spectrum, which in toluene-*d*₈ occurs at 143.14 ppm. Addition of 1 equiv of **13** to a toluene solution of C₆₀ results in a red solution, characteristic of the formation of the host–guest complex. Subsequent ¹³C NMR analysis reveals a 0.58 ppm downfield perturbation of the C₆₀ resonance. This downfield shift is consistent with the electron-deficient fullerene interacting with the electron-rich sulfur donors of the dithiocarbamate groups. This charge-transfer system results in a greater electron density residing on the fullerene when it is bound within the central cavity, leading to the downfield shift in the NMR signal. It is also further evidence that this is the method of coordination of the guest and not through a π – π stacking interaction with the resorcinarene subunits. This is also consistent with the fact that the metal center affects the binding constants of the complexes with fullerenes.

(20) The circular diameter was estimated via space filling CPK molecular model representations based on the crystal structures of the zinc and cadmium assemblies.

(21) Suzuki, T.; Nakashima, K.; Shinkai, S. *Chem. Lett.* **1994**, *23*, 699–702.

(22) Atwood, J. L.; Koustantonis, G. A.; Raston, C. L. *Nature* **1994**, *368*, 299–305.

(23) (a) Haino, T.; Yanase, M.; Fukazawa, Y. *Angew. Chem., Int. Ed. Engl.* **1997**, *36*, 259–260. (b) Yanase, M.; Haino, T.; Fukazawa, Y. *Tetrahedron Lett.* **1999**, *40*, 2781–2784. (c) Matsubara, H.; Shimura, T.; Hasegawa, A.; Semba, M.; Asano, K.; Yamamoto, K. *Chem. Lett.* **1998**, *27*, 1099–1100.

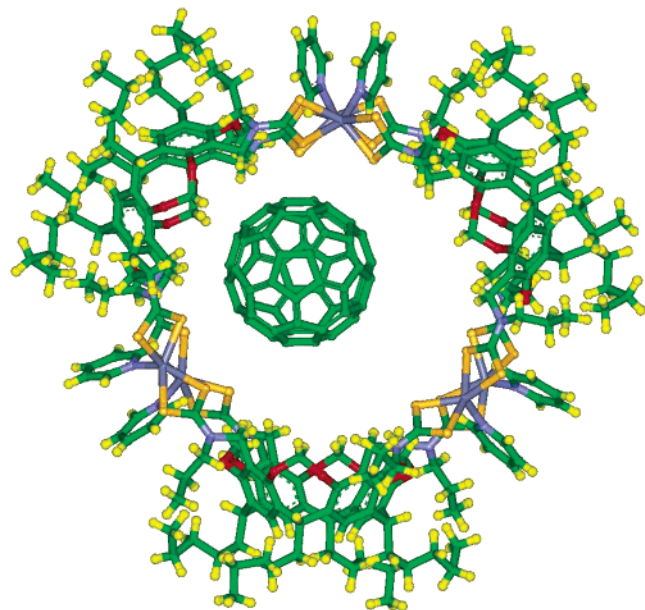
(24) Yoshida, Z.; Takekuma, H.; Takekuma, S.; Matsubara, Y. *Angew. Chem., Int. Ed. Engl.* **1994**, *33*, 1597–1599.

(19) Hynes, M. J. *J. Chem. Soc., Dalton Trans.* **1993**, 311–312.

Table 4. Electrochemical Data for C₆₀ in the Absence and Presence and Absence of 1.0 equiv of **13**^a

		wave 1 (V)	wave 2 (V)	wave 3 (V)
C ₆₀	<i>E</i> _{1/2}	-0.83	-1.24	-1.74
	<i>E</i> _{pc}	-0.90	-1.32	-1.83
	<i>E</i> _{pa}	-0.73	-1.14	-1.66
C ₆₀ plus 13	<i>E</i> _{1/2}	-0.83	-1.25	-1.76
	<i>E</i> _{pc}	-0.91	-1.34	-1.87
	<i>E</i> _{pa}	-0.73	-1.14	-1.66

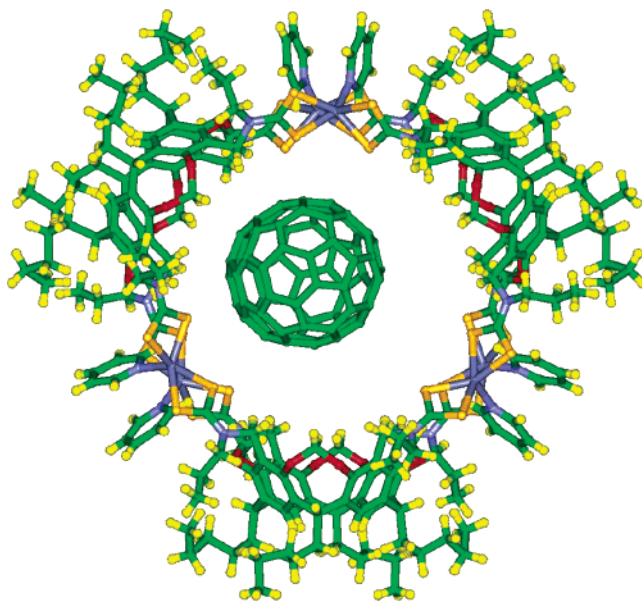
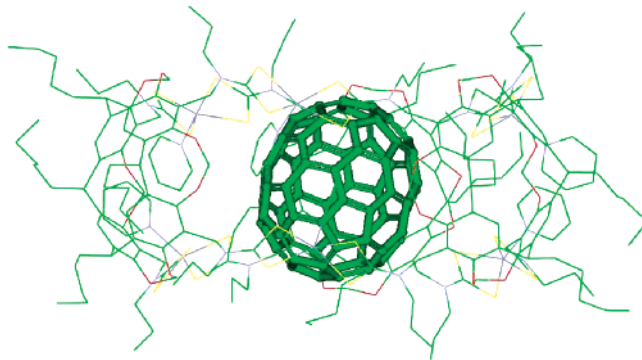
^a 85:15 toluene/MeCN containing 0.1 M TBABF₄, working electrode glassy carbon, scan rate 100 mV s⁻¹, {Ag/Ag⁺} reference electrode, errors ±5 mV.

**Figure 8.** Molecular mechanically determined structure of **11** with C₆₀ bound within the central cavity. Dark blue, zinc; dark yellow, sulfur; blue, nitrogen; red, oxygen; green, carbon; yellow, hydrogen.

Further evidence for C₆₀ binding was provided by electrochemical investigations. The first three reduction waves of C₆₀ were monitored upon addition of 1 equiv of **13** by cyclic and square voltammetry. Table 4 shows that, although addition of **13** does not result in a discernible change in the first reduction wave of C₆₀, it does lead to a 10 and 20 mV cathodic shift for the second and third reduction waves, respectively. This observation serves to illustrate that reduction of the fullerene becomes more difficult when it is bound inside the electron-rich cavity of **13**.²⁵ Due to the low solubility of C₆₀ it was not possible to examine the effect of adding excess fullerene to the electrochemical solution.

Molecular Modeling Studies of Hexanuclear Complexes.

The zinc(II) and cadmium(II) hexanuclear complexes **11**–**16** contain two-dimensional cavities that can readily accommodate both C₆₀ and C₇₀. The binding phenomenon was examined by placing the fullerenes within the cavity of **11** and performing molecular mechanics calculations with the Cerius2²⁶ program and the Universal force field.²⁷ The atoms were charged using the Qeq method. In both cases, on geometry optimization the guest molecule proved to be too small to be centered within

**Figure 9.** Molecular mechanically determined structure of **11** with C₇₀ bound within the central cavity. Dark blue, zinc; dark yellow, sulfur; blue, nitrogen; red, oxygen; green, carbon; yellow, hydrogen.**Figure 10.** Molecular mechanically determined structure of **11** with C₇₀ bound within the central cavity (side view). Dark blue, zinc; dark yellow, sulfur; blue, nitrogen; red, oxygen; green, carbon; yellow, hydrogen.

the cavity and was found at one end of the macrocycle. This resulted in close contacts with four of the six metal coordination spheres, with C···S distances of less than 4.0 Å (Figure 8). As expected, both guest molecules approached the sulfur atoms of the macrocycle, which were more open to close contacts.

The distances to the other two metal coordination spheres were very much larger, with the closest C···S contact being 5.8 Å. This close proximity of sulfur atoms to the guest C₆₀ molecule, which is illustrated in Figure 8, suggests that the electronic character of the dtc sulfur atoms, which is affected by the choice of metal ion, may dictate the strength of binding to the electron-deficient C₆₀ fullerene guest species. This is in agreement with the differing association constant values observed with the zinc(II) and cadmium(II) hexanuclear assemblies (Table 2).

A similar result was obtained through modeling the association of C₇₀ with the zinc(II) hexanuclear complex **11**. Again, the guest molecule was in closer proximity to four of the metal coordination spheres than the other two metal centers (Figures 9 and 10). One feature of the association of the elongated fullerene is that this guest is approximately the same height as the cavity of the host molecule (Figure 10). This results in the

(25) Boulas, P. L.; Gomez-Kaifer, M.; Echegoyen, L. *Angew. Chem., Int. Ed.* **1998**, *37*, 216–247.

(26) *Cerius2*, v3.5; Molecular Simulations Inc.: San Diego, CA, 1999.

(27) Rappe, A. K.; Casewit, C. J.; Colwell, K. S.; Goddard, W. A., III; Skiff, W. M. *J. Am. Chem. Soc.* **1992**, *114*, 10024–10035.

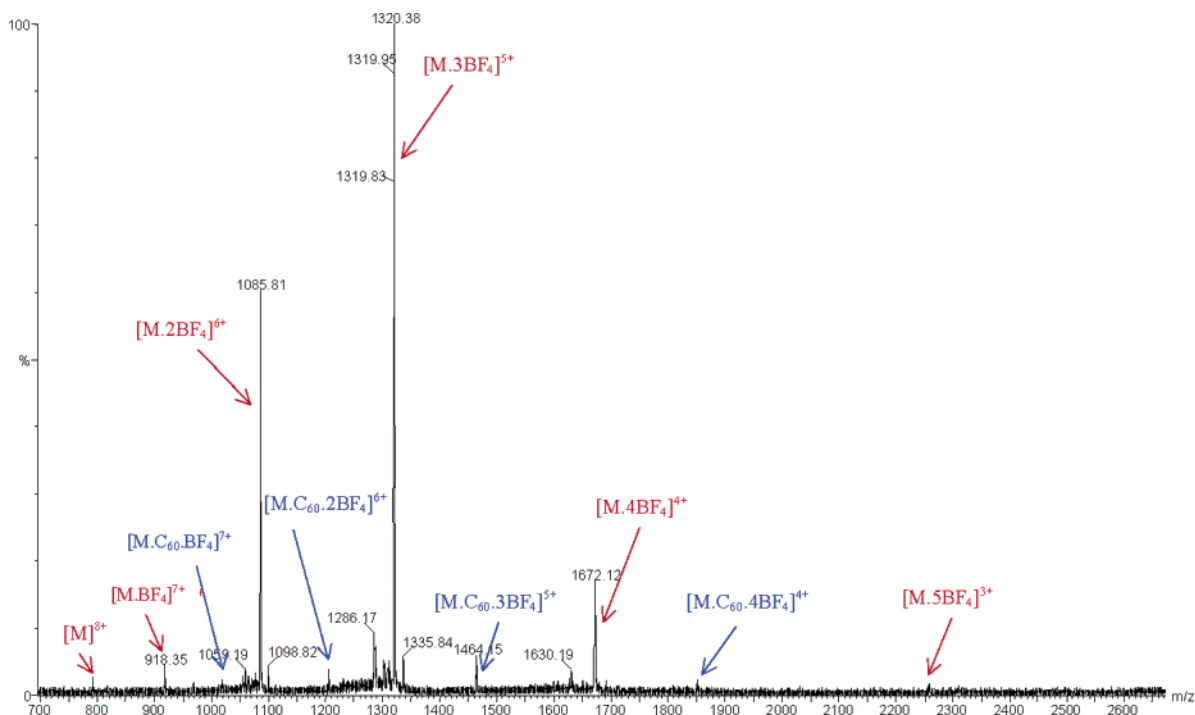


Figure 11. Electrospray mass spectrum of **9** and C_{60} after 10 min (oxidized in situ by $NOBF_4$).

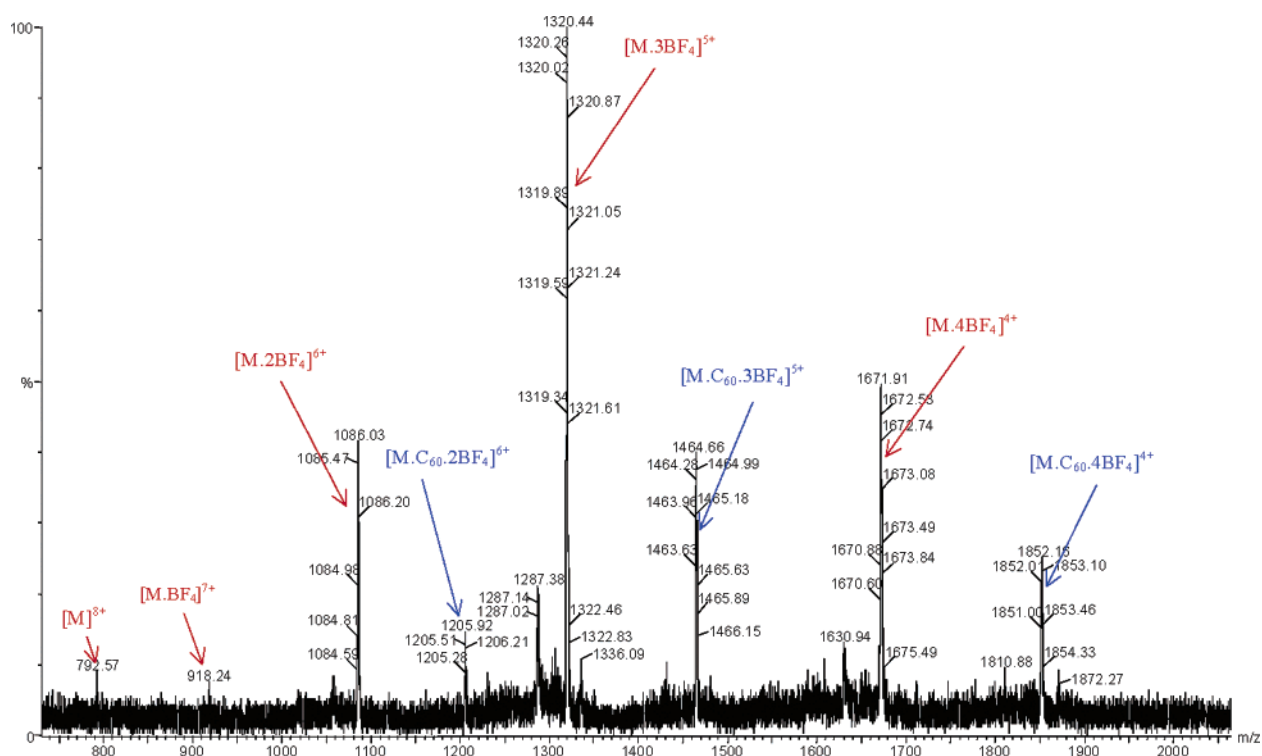


Figure 12. Electrospray mass spectrum of **9** and C_{60} after 1 h (oxidized in situ by $NOBF_4$).

majority of the outer carbon atoms also interacting with the host molecule. This increased enthalpic favorability is not, however, reflected in the corresponding stability constants due to the relative loss of rotational entropy upon the binding of C_{70} in comparison to the spherical C_{60} (Tables 2 and 3).

C_{60} Binding by Octanuclear Copper(II) Assemblies. The octanuclear copper(II) dithiocarbamate resorcinarene structures (Figure 1) possess nanosized internal dimensions, potentially large enough for the inclusion of a large guest species, such as

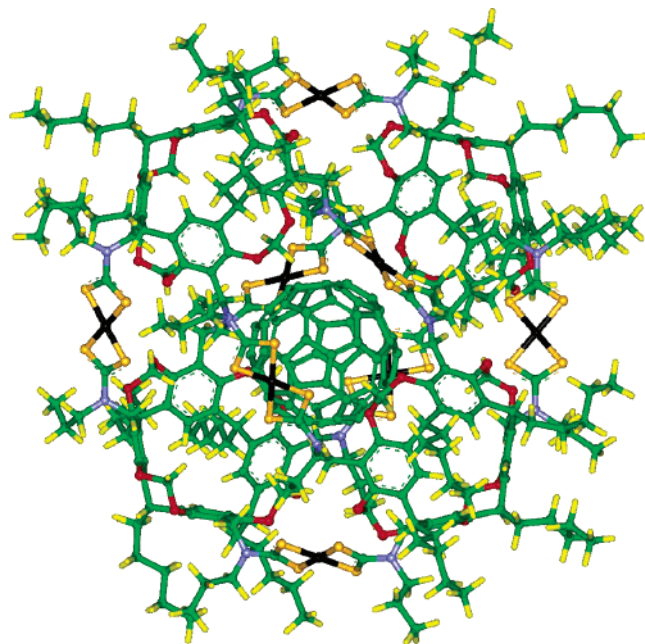
C_{60} . However, entrance to this cavity is restricted, since its portals are too small to allow such a large guest molecule to pass through them into the center. It may, however, be possible to utilize the lability of the copper(II) dithiocarbamate bond to enable guest encapsulation to take place. Such lability has previously been noted in first row transition metal dtc complexes^{28,29} with ligand exchange reactions having been observed.^{10a,30}

ESMS was used to investigate the possibility of binding C_{60}

Table 5. Electrochemical Data for the Cu(II)/(III) Oxidation in Octanuclear Hosts

	$E_{1/2}$ (V)	E_{pc} (V)	E_{pa} (V)
8	0.11	0.01	0.21
9	0.12	0.02	0.23
10	0.12	0.04	0.20

^a 1:1 CH₂Cl₂/MeCN containing 0.1 M TBABF₄, working electrode glassy carbon, scan rate 100 mV s⁻¹, {Ag/Ag⁺} reference electrode, errors estimated at ±5 mV.

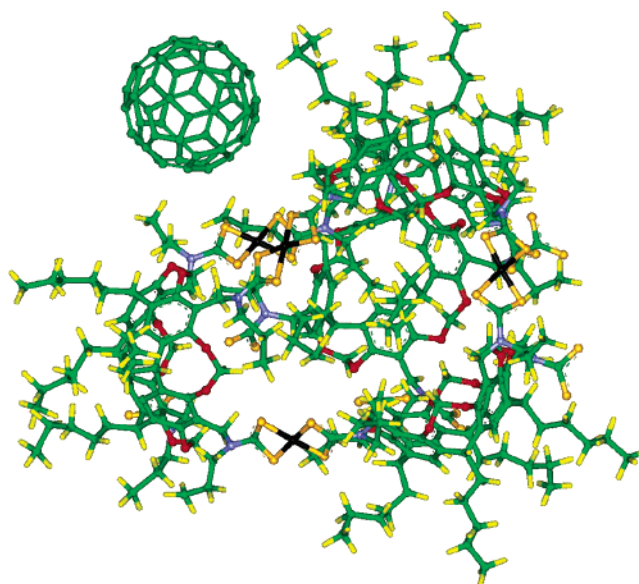
**Figure 13.** Molecular mechanically determined structure of **8** with C₆₀ in the cavity. Dark blue, copper; dark yellow, sulfur; blue, nitrogen; red, oxygen; green, carbon; yellow, hydrogen.

by the copper(II) assembly **9**. An equimolar solution of C₆₀ and **9** was prepared in an acetonitrile–dichloromethane–toluene (18:1:1) solution, and a sample of the mixture was injected into the mass spectrometer at regular intervals, following the injection of the oxidant NOBF₄. Overtime, significant peaks began to emerge for the presence of C₆₀ adducts with the octanuclear host (Figure 11).

Interestingly, only molecular ions for a 1:1 complex were observed, which increased in intensity overtime (Figure 12), suggesting C₆₀ encapsulation within the nanostructure as opposed to external association where multiple adducts would be expected without any time dependence. After 24 h no further change in the ESMS spectrum was observed suggesting equilibrium had been reached.

C₆₀ binding experiments using a 10 equiv excess of C₆₀ gave rise to a similar ESMS spectrum after just 1 h to that observed with 1 equiv after 24 h, implying the tetramer is indeed including the electron deficient fullerene within its electron-rich copper(II) dtc cavity via the lability of the copper(II)–dtc coordinate bonds.

Electrochemical investigations reveal that the copper(II) dtc complexes **8–10** undergo a single reversible copper(II)/(III) eight electron oxidation (Table 5). This suggests that all of the

**Figure 14.** Resulting theoretical structure of **10** after 100 ps in which the octanuclear complex had broken up and the C₆₀ was situated outside the cavity.

copper(II) centers behave independently of one another, being oxidized in one step. The addition of C₆₀ to the electrochemical solutions of the hosts did not, unfortunately, significantly perturb the respective oxidation waves.

This possible encapsulation of fullerene guests by the octanuclear cage complexes was further examined by molecular modeling. The guest molecules C₆₀ and C₇₀ were placed within the cavity of **8**, and molecular mechanics calculations showed that the host molecules could readily adapt to form stable complexes with the guest molecules surrounded by the host (**8**) (Figure 13).

However, molecular mechanics calculations showed that, even at 3000 K, the cavity was not flexible enough to allow the guest molecule to enter or depart the cavity. We conclude that, to allow guest species to enter (or exit) the cavity, one or more of the labile copper–dithiocarbamate bonds must break. Several simulations were carried out with a differing number of broken bonds. For a starting model, four copper atoms were removed from the C₆₀-bound structure in Figure 13 and a molecular mechanics simulation was carried out. Figure 14 shows the resulting structure after 100 ps in which the octanuclear complex had broken up and the C₆₀ was situated outside the cavity.

Conclusions

A selection of polymetallic resorcinarene based nanosized host assemblies has been prepared via metal directed assembly of dithiocarbamate functionalized cavitand structural frameworks. The stereochemical coordination preference of the transition metal used dictates the oligomeric type of the assembly that is adopted. With copper(II), octanuclear dithiocarbamate complexes were isolated, with single-crystal X-ray structural analysis revealing one such assembly to be that of a flattened tetrahedron. Chemical oxidation afforded the corresponding octacationic copper(III) complexes, where an X-ray crystal structure determination displayed a similar tetrahedral shaped arrangement of the cavitand components, linked together by approximately square planar copper(III) dithiocarbamate moieties. There is also evidence that analogous gold(III), nickel-

(28) Sachinidis, J.; Grant, M. W. *Aust. J. Chem.* **1981**, *34*, 2195–2215.

(29) Moriyasu, M.; Hashimoto, Y. *Bull. Chem. Soc. Jpn.* **1980**, *53*, 3590–3595.

(30) Beinrohr, E.; Garaj, J. *Collect. Czech. Chem. Commun.* **1980**, *45*, 1785–1792.

(II), and palladium(II) complexes also adopt an octanuclear, tetrameric structure. This suggests that this is the thermodynamically favored assembled product for transition metals with square planar geometric preferences. By contrast, with the group 12 metals, zinc(II) and cadmium(II) trimeric hexanuclear cavitand architectures are produced. X-ray crystallographic studies showed that those architectures possess cavities with complementary dimensions to the fullerenes C_{60} and C_{70} .

Strong 1:1 complexes are formed with fullerenes, where, despite similar cavity dimensions, the cadmium hexanuclear assemblies were found to be the superior host systems. Other techniques, such as electrochemistry, ^{13}C NMR spectroscopy, and molecular modeling also suggest that it is the electronic character of the dithiocarbamate sulfur donor atoms which, affected by the nature of the metal ion, dictate the strength of binding to the electron-deficient fullerene guest species.

ESMS provided evidence for the encapsulation of C_{60} by the copper(II) octanuclear assemblies. Structural data used in conjunction with molecular modeling studies reveals it is the lability of the copper(II) dithiocarbamate bond that enables the C_{60} guest encapsulation to take place, as the entrance to the nanosized cavity is restricted by its portals being too small to allow such a large guest molecule to pass through.

Experimental Section

General Methods. Chemicals were purchased from Aldrich and used as received. Deionized water was used in all cases. 1H and ^{13}C NMR experiments were performed on Varian 300 MHz Mercury VX Works and 500 MHz Unity Plus spectrometers. Elemental analyses were carried out by the Inorganic Chemistry Laboratory Microanalysis Service, University of Oxford. Mass spectra were recorded using a Micromass LCT electrospray mass spectrometer. Typical settings were as follows: Capillary Voltage 3.2 kV, Sample Cone 40 V, Extraction Cone 10 V, RFLens 200, Desolvation Temperature 80 °C, Source Temperature 60 °C. Where nitrosium tetrafluoroborate is added to the sample, milder conditions are used, i.e., Capillary Voltage 3.2 kV, Sample Cone 20 V, Extraction Cone 6 V, Desolvation Temperature 60 °C, Source Temperature 40 °C.

Tetra(bromomethyl)resorcinarene cavitand **1** and {tetrakis(propylamino)methyl}resorcinarene cavitand **2** were synthesized according to literature preparations.¹² The synthesis of the analogous tetrakisamines **3** and **4** are described in the Supporting Information. The tetrakis-dithiocarbamate salts **5–7** were not isolated. The syntheses of the multinuclear complexes of **11**, **12**, **13**, and **14** have been previously reported.¹¹

Cu(II) Dithiocarbamate-Based (Propylamino)resorcinarene Octanuclear Complex (8). {Tetrakis(propylamino)methylresorcinarene} cavitand **2** (1.00 g, 0.92 mmol) was dissolved in a THF/ H_2O (2:1, 100 mL) solution and KOH (0.22 g, 3.96 mmol) and CS_2 (0.29 g, 4.00 mmol) added sequentially. $Cu(OAc)_2$ (0.41 g, 2.20 mmol) was then added to the yellow solution, and the reaction mixture stirred at room temperature for 18 h. The resulting fine, dark brown powder was filtered and recrystallized from $CH_2Cl_2/EtOH$ yielding black crystals, which were collected and dried in vacuo (0.88 g, 63%). ESMS(m/z) with $Cu(OTf)_2$: 1070.3 [$M \cdot 2OTf$]⁶⁺, 1313.3 [$M \cdot 3OTf$]⁵⁺, 1677.3 [$M \cdot 4OTf$]⁴⁺. Elemental Analysis calcd for $C_{288}H_{384}N_{16}O_{32}S_{32}Cu_8 \cdot 2CH_2Cl_2$: C, 55.66; H, 6.25; N, 3.58. Found: C, 55.51; H, 6.05; N, 3.43.

Cu(II) Dithiocarbamate-Based (Butylamino)resorcinarene Octanuclear Complex (9). Synthesized by an analogous method to **8** using **3** (1.00 g, 0.86 mmol), KOH (0.22 g, 3.96 mmol), CS_2 (0.29 g, 4.00 mmol), and $Cu(OAc)_2$ (0.41 g, 2.20 mmol) (0.82 g, 62%). ESMS(m/z) with $NOBF_4$: 792.6 [M]⁸⁺, 918.4 [$M \cdot BF_4$]⁷⁺, 1085.6 [$M \cdot 2BF_4$]⁶⁺, 1320.3 [$M \cdot 3BF_4$]⁵⁺, 1671.9 [$M \cdot 4BF_4$]⁴⁺, 2258.1 [$M \cdot 5BF_4$]³⁺. Elemental

Analysis calcd for $C_{304}H_{416}N_{16}O_{32}S_{32}Cu_8 \cdot 2CH_2Cl_2$: C, 56.45; H, 6.50; N, 3.44. Found: C, 56.53; H, 6.28; N, 3.42.

Cu(II) Dithiocarbamate-Based (Hexylamino)resorcinarene Octanuclear Complex (10). Synthesized by an analogous method to **8** using **4** (1.00 g, 0.79 mmol), KOH (0.22 g, 3.96 mmol), CS_2 (0.29 g, 4.00 mmol), and $Cu(OAc)_2$ (0.41 g, 2.20 mmol) (0.87 g, 65%). ESMS(m/z) with $NOBF_4$: 1160.5 [$M \cdot 2BF_4$]⁶⁺, 1410.0 [$M \cdot 3BF_4$]⁵⁺, 1784.2 [$M \cdot 4BF_4$]⁴⁺. Elemental Analysis calcd for $C_{336}H_{480}N_{16}O_{32}S_{32}Cu_8 \cdot 2CH_2Cl_2$: C 62.96; H 7.57; N 3.48. Found: C 62.68; H 7.37; N 3.38.

Zn(II) Dithiocarbamate-Based (Hexylamino)resorcinarene Hexanuclear Complex (13). Synthesized in an analogous method to that of **8** using {tetrakis(hexylamino)methylresorcinarene} cavitand **4** (1.00 g, 0.86 mmol) by the addition of $Zn(OAc)_2$ (0.41 g, 2.0 mmol). The resulting cream solid was redissolved in pyridine and precipitated by the addition of water and recrystallized from $CHCl_3/EtOH$ (0.62 g, 52%). 1H NMR (300 MHz, $CDCl_3$) δ_H : 8.85 (12H, s, pyH), 7.80 (6H, s, pyH), 7.44 (12H, s, pyH), 7.12 (12H, s, ArH), 5.85 (12H, m(br), $OCH_2[H_{outer}]$), 4.76 (12H, s, $ArCHCH_2$), 4.35–3.54 (36H, m(br), $OCH_2[H_{inner}]$ and $ArCH_2$), 2.21 (24H, s, CH_2), 1.71–1.23 (192H, m, CH_2), 0.90 (72H, m, CH_3). Elemental Analysis calcd for $C_{282}H_{390}N_{18}O_{24}S_{24} \cdot Zn_6 \cdot 8CHCl_3 \cdot 8 \frac{1}{2}H_2O$: C, 52.52; H, 6.22; N, 3.80. Found: C, 52.76; H, 6.47; N, 3.50.

Cd(II) Dithiocarbamate-Based (Hexylamino)resorcinarene Hexanuclear Complex (16). Synthesized in an analogous method to that of **8** using {tetrakis(hexylamino)methylresorcinarene} cavitand **8** (1.00 g, 0.86 mmol) by the addition of $Cd(OAc)_2$ (0.41 g, 2.0 mmol). The resulting cream solid was redissolved in pyridine and precipitated by the addition of water and recrystallized from $CHCl_3/EtOH$ (0.72 g, 62%). 1H NMR (300 MHz, $CDCl_3$) δ_H : 8.65 (12H, s, pyH), 7.69 (6H, s, pyH), 7.30 (12H, s, pyH), 7.08 (12H, s, ArH), 5.85 (12H, m(br), $OCH_2[H_{outer}]$), 4.72–3.80 (48H, m(br), $ArCHCH_2$ and $OCH_2[H_{inner}]$ and $ArCH_2$), 2.16 (24H, s, CH_2), 1.69 (48H, m, CH_2), 1.33 (144H, s(br), CH_2), 0.89 (72H, m, CH_3). Elemental Analysis calcd for $C_{282}H_{390}N_{18}O_{24}S_{24} \cdot Cd_6 \cdot 8CHCl_3 \cdot 4H_2O$: C, 50.57; H, 5.94; N, 3.65. Found: C, 50.55; H, 5.94; N, 3.35.

Au(III) Dithiocarbamate-Based (Butylamino)resorcinarene Octanuclear Complex (17). The direct reaction method was performed via an analogous method to that undertaken in **9**. The transmetalation reaction occurred as follows: 1 equiv of the octanuclear Cu(II) complex **9** (10.0 mg, 1.6 μ mol) was dissolved in $CH_2Cl_2/MeCN$ (1:1, 50 mL, dry) and stirred under N_2 . 16 equiv of $KAuCl_4$ were added to the dark brown solution, which immediately turned golden yellow. The solution was stirred for a further 10 min and analyzed by mass spectrometry. ESMS(m/z): 1685.1 [$M \cdot 3AuCl_4$]⁵⁺, 2190.8 [$M \cdot 4AuCl_4$]⁴⁺. Unfortunately, attempts to isolate an elementally pure complex were not successful.

Ni(II) Dithiocarbamate-Based (Butylamino)resorcinarene Octanuclear Complex (18). Synthesized using an analogous method to that for **9** by the addition of $Ni(OAc)_2$ (0.13 g, 0.5 mmol) forming a green crystalline solid (0.04 g, 12%). 1H NMR (300 MHz, $CDCl_3$) δ_H : 7.12 (16H, m, ArH), 6.30–5.86 (16H, m, $OCH_2[H_{outer}]$), 5.22–4.98 (16H, m, $OCH_2[H_{inner}]$), 4.73 (16H, m, CH), 4.12 (32H, m, CH_2), 3.42 (32H, m, CH_2), 2.21 (32H, s, CH_2), 1.32–1.15 (160H, m, CH_2), 0.91–0.72 (96H, m, CH_3). ^{13}C NMR (75.48 MHz, $CDCl_3$) δ_C : 207.57 (CS_2), 154.41, 153.71, 148.31, 138.97, 138.16 (ArC), 121.05, 119.52, 46.87, 36.50, 31.81, 29.66, 28.46, 27.37, 22.67, 19.94, 19.71 (CH_2), 14.04, 13.57 (CH_3). Elemental Analysis calcd for $C_{304}H_{416}N_{16}O_{32}S_{32}Ni_8 \cdot 4CH_2Cl_2 \cdot 7H_2O$: C, 54.66; H, 6.52; N, 3.31. Found: C, 54.80; H, 6.29; N, 3.32.

Pd(II) Dithiocarbamate-Based (Butylamino)resorcinarene Octanuclear Complex (19). Synthesized using an analogous method to that for **9** by the addition of K_2PdCl_4 (0.41 g, 1.23 mmol) forming a yellow crystalline solid (0.58 g, 9%). 1H NMR (300 MHz, $CDCl_3$) δ_H : 7.19 (16H, m, ArH), 6.18–5.90 (16H, m, $OCH_2[H_{outer}]$), 5.33–5.10 (16H, m, $OCH_2[H_{inner}]$), 4.82–4.71 (16H, m, CH), 4.34–4.21 (32H, m, CH_2), 3.14 (32H, m, CH_2), 2.21 (32H, s, CH_2), 1.39–1.13 (160H,

m, CH₂), 0.89 (96H, m, CH₃). Elemental Analysis calcd for C₃₀₄H₄₁₆N₁₆O₃₂S₃₂Pd₈: C, 54.63; H, 6.27; N, 3.35. Found: C, 55.03; H, 6.54; N, 3.24.

X-ray Crystallography. The hexanuclear complexes **11**, **12**, **14**, and **15** were characterized by single-crystal X-ray crystallography, and their structures have been reported elsewhere¹¹ and deposited in the CCDC (reference codes CUPKUT, MAKVUPCd, MAKVID, and MAKVOJ).

The single-crystal experiment reported here was performed using a Bruker SMART 1K CCD area detector equipped with an Oxford Cryosystems Cryostream on Station 9.8 of the Synchrotron Radiation Source, CCLRC Daresbury Laboratory.³¹ Data were collected at a wavelength of 0.6887 Å and a temperature of 150(2) K.

Crystal data for **10**: C₃₃₆H₄₈₀N₁₆O₃₂S₃₂Cu₈, M = 6789.60, brown block, 0.36 × 0.22 × 0.10 mm³, triclinic, space group $P\bar{1}$, $a = 35.223(5)$ Å, $b = 35.405(5)$ Å, $c = 42.733(6)$ Å, $\alpha = 94.974(2)^\circ$, $\beta = 112.209(2)^\circ$, $\gamma = 89.982(2)^\circ$, $V = 49121$ Å³, $Z = 4$, $\rho_{\text{calcd}} = 0.918$ g/cm⁻³, $\mu = 0.521$ mm⁻¹. 99 767 reflections measured, 51 833 unique ($R_{\text{int}} = 0.0478$), 26664 > 2 $\sigma(I)$ were used to refine 3897 parameters with 2396 restraints to $R1$ ($wR2$) = 0.1762 (0.4675) for $I > 2\sigma$. The crystal diffracted extremely weakly: as a result the data were cut at 32° 2 θ , as, above this, the average I/σ was less than 2 and thus considered unobserved. The structure was solved by direct methods³² and refined with only copper and sulfur atoms allowed to refine with anisotropic displacement parameters.³³ All non-hydrogen atoms were found in the difference map except for several carbons in the highly disordered -C₆H₁₃ and -C₅H₁₁

groups which were therefore omitted from the refinement. Geometrical and displacement parameter restraints were applied to the -C₆H₁₃ and -C₅H₁₁ groups.

Crystallographic data (excluding structure factors) for this structure has been deposited with the Cambridge Crystallographic Data Centre as supplementary publication number CCDC 268180. Copies of the data can be obtained free of charge on application to CCDC, 12 Union Road, Cambridge, CB2 1EZ, UK (Fax: (+44) 1223 336 033. E-mail: deposit@ccdc.cam.ac.uk).

Acknowledgment. Financial support for this work was kindly provided by AWE Aldermaston (O.D.F.) and a EPSRC post-doctoral fellowship (O.D.F.). We also thank EPSRC and Johnson Matthey for a CASE studentship (J.C.). We would also like to thank Johnson Matthey for the generous loan of gold, palladium, and platinum salts. We acknowledge the provision of time on DARTS, the UK national synchrotron radiation service at the CCLRC Daresbury Laboratory, through funding by EPSRC.

Supporting Information Available: ¹H NMR spectra of **9**, **18**, and **19** and synthetic protocols for the synthesis of organic precursors **3** and **4**. This material is available free of charge via the Internet at <http://pubs.acs.org>.

(31) Cernik, R. J.; Clegg, W.; Catlow, C. R. A.; Bushnell-Wye, G.; Flaherty, J. V.; Greaves, G. N.; Hamichi, M.; Burrows, I.; Taylor, D. J.; Teat, S. J. *J. Synchrotron Rad.* **1997**, *4*, 279–286.

(32) Sheldrick, G. M. *SHELXS-97. Acta Crystallogr., Sect. A* **1990**, *46*, 467–473.

JA060982T

(33) Sheldrick, G. M. *SHELXL-97*. Universität Göttingen: Germany, 1997.